2011 IEEE International Conference on Robotics and Automation
Shanghai International Conference Center
May 9-13, 2011, Shanghai, China

# Control of Upper-Limb Power-Assist Exoskeleton Based on Motion Intention Recognition

Weiguang Huo, Jian Huang*, *Member, IEEE,* Yongji Wang, Jun Wu, Lei Cheng

*Abstract*—**Recognizing the user motion intention plays an important role in the study of power-assist robots. An intention-guided control strategy is proposed for the upper-limb power-assist exoskeleton. A force sensor system comprised of force sensing resistors (FSRs) is designed to online estimate the motion intention of user upper limb. A new concept called "intentional reaching direction (IRD)" is proposed to quantitatively describe this intention. Both the state model and the observation model of IRD are obtained by enumerating the upper limb behavior modes and analyzing the relationship between the measured force signals and the motion intention. Based on these two models, the IRD can be online inferred by applying filtering technology. Guided by the estimated IRD, an admittance control strategy is assumed to control the motions of three DC motors in the joints of the robotic arm. The effectiveness of the proposed approaches is finally confirmed by the experiments on a 3-DOF robotic exoskeleton.**

## I. INTRODUCTION

As many countries step into the aging society rapidly, more and more elders suffer from deficits of motor function or disability of the upper limb. Recently, the power-assist robot becomes a popular research topic because it can be used to improve the motion ability of the elderly. The recognition of user motion intention plays an important role in the study of power-assist robots. From the point of view of the control system of robot, the user motion intention provides a reference trajectory for the robot motion controller. Therefore, the more accurately the motion intention is recognized, the more satisfactory control performance of the robot may be obtained.

So far, there are plentiful power-assist robotic applications involved with motion intention recognition. HAL system [1-3] of Tsukuba University is a lightweight power-assist robot with DC motors at the knees and hip. In the HAL system, EMG electrodes on human's leg muscles and ground reaction force sensors were used to estimate human motion intention. Yamamoto, Ishii et. al. [4] proposed a standing alone wearable power assisting suit. In their study, the user motion intention was recognized by measuring the hardness of corresponding muscles. Chen, Yu et. al. [5] introduced a walking power-assist leg (WPAL) with a method based on human-robot interaction force to understand the user motion intention. Rosen et al. presented an EMG-based power exoskeleton system [6]. Kiguchi et. al. [7-8] developed several robotic exoskeletons to assist motion of physically weak persons. These robotic exoskeletons were controlled based on the EMG signals, which are important signals to understand how the user intends to move.

Although the user motion intention is very important in power assist robots, there are few researchers explicitly discussed its modeling and estimation problem. In our previous study [9], the concept of user intentional direction was proposed and the corresponding motion intention estimation problem was investigated. In the study of motion intention recognizing approaches, the EMG-based methods are widely applied. However, the EMG signals are easily influenced by the location of electrodes, the thickness of fattiness, the body temperature and the perspiration. Meanwhile, the information of the EMG signals is so large that a complicated preprocessing procedure is required before using them as the control input [5]. On the other hand, the power-assist robot applications for upper limb are relatively less than that for the lower limb of user. The reason might rely on the fact that the motion of upper limb is more flexible.

In this study, we propose an intention-guided control strategy for upper-limb power-assist exoskeleton based on online estimating the user motion intention. A 3-DOF robotic exoskeleton is designed to test our control approach. To avoid the problems of EMG-based intention recognition approaches, a force sensor system comprised of force sensing resistors (FSRs) is designed to online estimate the motion intention. A new concept called "intentional reaching direction (IRD)" is proposed to quantitatively describe the motion intention of user upper limb. By enumerating the upper limb behavior modes, a hybrid state model of IRD is obtained. The observation model of IRD is derived from analyzing the relationship between the measured force signals and the actual IRD. Based on these two models, the IRD can be online inferred by applying filtering technology. Guided by the estimated IRD, an admittance control strategy is assumed to control the motions of three DC motors in the joints of the robotic arm.

This work is partially supported by Hi-tech Research and Development Program of China under Grant 2007AA04Z204 and Grant 2008AA04Z207, and in part by the Natural Science Foundation of China under Grant 60975058 and 61075095. The work is also supported by State Key Laboratory of Robotics and System (HIT).

Weiguang Huo, Jian Huang, Yongji Wang, Jun Wu are with the Key Laboratory of Image Processing and Intelligent Control, Department of Control Science and Technology, Huazhong University of Science and Technology, Wuhan, 430074, China, huang_jan@mail.hust.edu.cn. Lei Cheng is with the Engineering Research Center of Metallurgical Automation and Measurement Technology, Ministry of Education in China, Wuhan University of Science and Technology, Wuhan, 430081, China.

## II. Modeling and Estimation of Upper Limb Motion Intention

### A. *Intentional reaching direction (IRD) and its state model*

The reaching-out movement may be the most important motion of human upper limb in the daily life. Many daily activities, e.g. dining and washing, are composed of a series of reaching-out movement. It should be pointed out that the motion trajectory of the end of upper limb (i.e. the hand) characterizes an intentional reaching-out movement. Therefore, it can be used to quantitatively describe the motion intention of human upper limb. An important concept is then introduced as follows, which is similar to the intentional direction (ITD) proposed in our previous study [9].

**Definition 1.** The direction to which a person's hand intends to move is referred to as the intentional reaching direction (IRD).

As shown in Fig. 1, the IRD can be evaluated by two angles $\rho_{s1}$ and $\rho_{s2}$. During the movement of upper limb, the IRD will be arbitrarily adjusted by the human. In the rest of paper, we use a time-dependent 2-tuple to denote the IRD, which is given by

$$\tilde{S}(n) = \langle \rho_{s1}(n), \rho_{s2}(n) \rangle \tag{1}$$

where $n$ is used to denotes the time stamp.

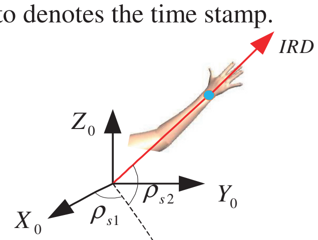


Fig.1. IRD in the reference coordinate system

To fully formulate the motion intention, it is required to obtain the dynamic model of IRD. The first thing we should do is to enumerate possible motion modes of the upper limb. Although there are various motion modes in the motion of human upper limb, only several of them are fundamental and often used in the daily life, e.g, grasping a cup or opening the door. In this study, four simple upper limb motion modes are considered, which are listed in TABLE I. The transition diagram of four modes is also illustrated by Fig.2. In the following, we use $\tilde{I}(n)$ to represent the current motion mode of the upper limb.

TABLE I. POSSIBLE MOTION MODES

| Mode | Description |
|---|---|
| I | Stop |
| II | Bending and stretching around single joint. |
| III | Moving straight |
| IV | Moving along an arc |

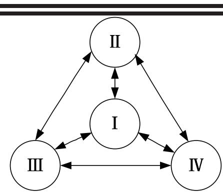


Fig.2. Transition diagram of the possible motion modes.

Although mode transition is possible to occur between any two of the four motion modes, in practice, mode I "Stop" is usually an intermediate state that connects any other two modes.

It is apparent that the dynamic model of IRD is different in different motion modes. Empirically, we have the following assumptions:

***Assumption 1***. In mode I, the IRD is assumed to be always zero.

***Assumption 2***. In model II, the motion of arm is restricted by the structure of exoskeleton. Therefore, the evolution of IRD can be easily calculated using the Jacobian matrix of exoskeleton.

***Assumption 3***. In mode III, the IRD is supposed to be a constant.

***Assumption 4***. We assume that the upper limb moves very slow with the exoskeleton. Thus, the IRD is supposed to be changed with a nearly constant speed in mode IV.

Let us choose the two state variables $X$ and $X^m$ to be

$$\begin{aligned} X(n) &= \left[\rho_{s1}(n) \quad \rho_{s2}(n)\right]^{\mathrm{T}} \\ X^m(n) &= \left[\rho_{s1}(n) \quad \rho_{s2}(n) \quad \dot{\rho}_{s1}(n) \quad \dot{\rho}_{s2}(n)\right]^{\mathrm{T}}. \end{aligned} \tag{2}$$

In terms of the given assumptions, a hybrid state model of IRD is described by

$$\begin{cases} X(n+1) = A_{\sigma(n)} \cdot X(n), & \text{when } \sigma(n) \in \{I, II, III\} \\ X^m(n+1) = A_{\sigma(n)} \cdot X^m(n), & \text{when } \sigma(n) = IV \end{cases} \tag{3}$$

where $\sigma(n)$ denotes the different motion mode given by TABLE I. Note that the velocity of IRD is considered only in mode IV, which leads to a variable dimension hybrid state model. The state transition matrices are given by

$$A_I = \mathbf{0}_{2\times2},\ A_{II} = diag\left(a_1(t), a_2(t)\right),\ A_{III} = \mathbf{I}_{2\times2},$$
$$A_{IV} = \begin{bmatrix} 1 & 0 & T & 0 \\ 0 & 1 & 0 & T \\ 0 & 0 & 1 & 0 \\ 0 & 0 & 0 & 1 \end{bmatrix}. \tag{4}$$

where $\mathbf{0}$ and $\mathbf{I}$ are used to indicate the zero matrix and identity matrix respectively. $diag(\bullet)$ is used to denote the diagonal matrix. $T$ is the control period. Note that the time-dependent parameters $a_1(t)$ and $a_2(t)$ can be easily obtained from the Jacobian matrix of exoskeleton.

### B. *Force sensing system and the observation model of IRD*

In order to online estimate the motion intention of upper limb, a force sensing system is designed as shown in Fig.3.

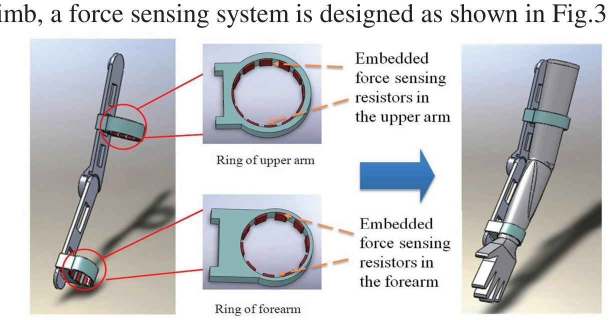


Fig.3. The force sensing system

The force sensing system consists of two wearable rings and two groups of force sensing resistors (FSRs), which are much cheaper than multi-axis force sensors. In this study, the wearable rings are made of thermoplastic material, which are used for fixing the human upper limb on the power-assist exoskeleton. Two groups of FSRs are fixed on the inner surfaces of the wearable rings (see Fig.3). If the FSRs are sufficiently sensitive, a slight motion of the user upper limb can be detected. Generally, even a weak old person is able to perform such slight motion when he/she does intend to move the upper limb. Hence, we can use the force signals to infer the motion intention of the human upper limb.

Apart from the force component indicating the motion intention, the measured forces also include the force components caused by the gravity of the upper limb. To compensate the effects of gravity, the static force model of the upper limb in a relaxed state is required.

For simplicity, we assume that the number of DOF of the upper limb is four. That is, the shoulder joint has 3 DOF while the elbow joint has 1 DOF. The coordinate system of the human upper limb is shown by Fig.4.

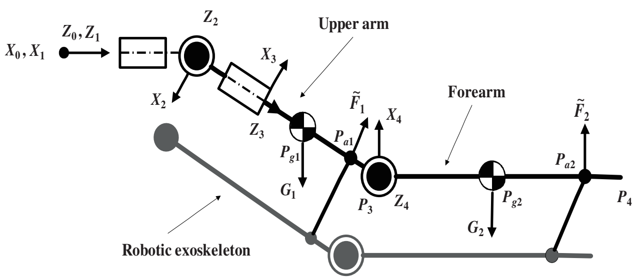


Fig.4. The coordinate system of human upper limb.

*1) Compensation for the gravity of upper limb*

When the user relaxes his/her arm, all the four joints of the upper limb shown in Fig. 4 are supposed to be free. We assume that the weight of upper limb is a constant. To hold the arm in a fixed position, the required static force to compensate the gravity of upper limb can be analyzed. Some notations are clarified first (see also Fig.4):

$\{X_0, Y_0, Z_0\}$ - the reference coordinate system of the human upper limb.

$\{X_i, Y_i, Z_i\}$ - the coordinate system of joint $i$ of human upper limb. ($i$=1, 2, 3, 4)

$G_i$ - the gravity of upper arm and forearm.

$\tilde{F}_1$, $\tilde{F}_2$ - the resultant forces exerted on the upper arm and forearm by the wearable rings.

$P_{g1}$, $P_{g2}$, $P_{a1}$, $P_{a2}$, $P_3$, $P_4$ - the position vectors .

We assume that the frictions between the wearable rings and the arm can be ignored. Thus, the resultant forces of the wearable rings acting on the upper arm and the forearm are described respectively in the corresponding coordinate systems {3} and {4} as follows:

$$ {}^3\tilde{F}_1 = [\tilde{F}_{1x}, \tilde{F}_{1y}, 0]^{\mathrm{T}} . \qquad (5)$$

$$ {}^4\tilde{F}_2 = [\tilde{F}_{2x}, 0, \tilde{F}_{2z}]^{\mathrm{T}} . \qquad (6)$$

In the reference coordinate system {0}, the gravity of the upper limb and the forearm are given by

$$ {}^0G_1 = [0, g_1, 0]^T . \qquad (7)$$

$$ {}^0G_2 = [0, g_2, 0]^T . \qquad (8)$$

In the coordinate system of joint 2 and joint 3, the gravities of the forearm and the upper arm are computed:

$$\begin{cases} {}^3G_1 = {}^3_2R\,{}^2_1R\,{}^1_0R\,{}^0G_1 \\ {}^4G_2 = {}^4_3R\,{}^3_2R\,{}^2_1R\,{}^1_0R\,{}^0G_2 \end{cases} . \qquad (9)$$

To maintain the static equilibrium, the required forces and torques are given by: [10]

$$\begin{cases} {}^if_i = {}^i_{i+1}R\,{}^{i+1}f_{i+1} \\ {}^in_i = {}^i_{i+1}R\,{}^{i+1}n_{i+1} + {}^iP_{i+1} \times {}^if_i \end{cases} \qquad (10)$$

where $f_i$ is the force exerted on link $i$ by $i$-1. $n_i$ is the torque exerted on link $i$ by $i$-1. ${}^i_{i+1}R$ is the rotation matrix describing frame $\{i + 1\}$ relative to frame $\{i\}$. ${}^i_{i+1}R$ is the position vector from joint $i$ to joint $i+1$.

Because all joints of upper limb are supposed to be free in a relaxed state, the dot products of the joints axis vectors with the moment vectors acting on the link all equal to zero.

$$\begin{cases} {}^4n_4\hat{Z}_4 = 0 \\ {}^3n_3\hat{Z}_3 = 0 \\ {}^2n_2\hat{Z}_2 = 0 \\ {}^1n_1\hat{Z}_1 = 0 \end{cases} \qquad (11)$$

To overcome the gravity, the required forces exerted on the human upper limb by the wearable rings can be obtained by solving the equations from (5) to (11). In the following, we use $\tilde{F}_1^*$ and $\tilde{F}_2^*$ to denote these forces. Obviously, the measured force components that truly reflect the motion intention are given by

$$\hat{F}_1 = \tilde{F}_1 - \tilde{F}_1^*,\ \hat{F}_2 = \tilde{F}_2 - \tilde{F}_2^* . \qquad (12)$$

*2) Observation model of IRD using force sensing system*

Although forces $\hat{F}_1$ and $\hat{F}_2$ reflect the user motion intention of upper limb, there still remains a problem of how to calculate the IRD. The shoulder and elbow joints are not free if $\hat{F}_1$ and $\hat{F}_2$ are not zero. In this case, the torques acted on the joints by the user are also observations of the motion intention. Based on the assumption that the user moves his/her upper limb in a slow constant speed, the joint toques can be calculated as follows [10]:

$$\begin{bmatrix} \hat{\tau}_1 \\ \hat{\tau}_2 \\ \hat{\tau}_3 \\ \hat{\tau}_4 \end{bmatrix} = \tilde{J}^{\mathrm{T}} \begin{bmatrix} \hat{F}_1 \\ \hat{F}_2 \end{bmatrix} \qquad (13)$$

where $\tilde{J}$ is a Jacobian-like matrix. $\hat{\tau}_i$ ($i$=1, 2,…, 4) are the torques acted on joint $i$ by the user corresponding to measured forces $\hat{F}_1$ and $\hat{F}_2$. To establish the relationship between the IRD and toques $\hat{\tau}_i$, we propose two important assumptions:

***Assumption 5***. The desired joint rotation velocity is supposed to be proportional to the torque exerted on this joint. That is, we have

$$\hat{\omega}_i = d_i \cdot \hat{\tau}_i,\ i = 1,2,3,4. \quad (14)$$

where $\hat{\omega}_i$ are the desired rotation velocities of the joint $i$ of the human upper limb. $d_i$ are constant coefficients.

***Assumption 6***. For the same user, the ratio values including $d_2 / d_1$, $d_3 / d_1$ and $d_4 / d_1$ are constants no matter how he/she moves the upper limb.

According to the desired joint rotation velocities and the current joint angles, the resultant desired velocity of hand is given by

$$\hat{V}_h = J_h \cdot \left[\hat{\omega}_1 \quad \hat{\omega}_2 \quad \hat{\omega}_3 \quad \hat{\omega}_4\right]^{\mathrm{T}} \quad (15)$$

where $J_h$ is the Jacobian matrix of human upper limb. Obviously velocity $\hat{V}_h$ has the same direction as the IRD. From (13), (14) and (15) we can conclude the relationship between the measured forces and the human motion intention as follows:

$$\hat{V}_h = J_h \cdot diag(d_1, d_2, d_3, d_4) \cdot \tilde{J}^{\mathrm{T}} \cdot \begin{bmatrix} \hat{F}_1 \\ \hat{F}_2 \end{bmatrix}. \quad (16)$$

Let us suppose that representation of velocity $\hat{V}_h$ in the reference coordinate system is described by

$${}^0\hat{V}_h = \left[\hat{V}_{hx} \quad \hat{V}_{hy} \quad \hat{V}_{hz}\right]^{\mathrm{T}} \quad (17)$$

The observation value of IRD is then given by

$$\hat{S}(n) = \left\langle \rho_{o1}(n), \rho_{o2}(n) \right\rangle \quad (18)$$

where

$$\rho_{o1}(n) = \tan^{-1} \frac{\hat{V}_{hy}}{\hat{V}_{hx}} \quad (19)$$

$$\rho_{o2}(n) = \tan^{-1} \frac{\hat{V}_{hz}}{\sqrt{\hat{V}_{hx}{}^2 + \hat{V}_{hy}{}^2}} \quad (20)$$

Usually there are significant noises in the measured force signals. The observation model of IRD can be described by

$$\begin{cases} Z(n) = H \cdot X(n) + v(n), & \text{when } \sigma(n) \in \{I, II, III\} \\ Z(n) = H^m \cdot X^m(n) + v(n), & \text{when } \sigma(n) = IV \end{cases} \quad (21)$$

where

$$H = \mathbf{I}_{2\times 2} \quad H^m = \begin{bmatrix} 1 & 0 & 0 & 0 \\ 0 & 1 & 0 & 0 \end{bmatrix} \quad (22)$$

$v(n)$ is a combination of sensor noises and human upper limb moving habit, which can be assumed as a white noise for simplicity, i.e. $v(n) \sim N(0, R)$.

### *C. Online estimation of IRD*

In this section, we discuss the approach to online estimate the IRD from measured noisy forces $\tilde{F}_1$ and $\tilde{F}_2$ based on state and observation models (3) and (21). The first problem should be solved is how to detect the current motion mode. In this study, a rule-based method is assumed to estimate the mode $\tilde{I}(n+1)$ from the torques $\hat{\tau}_i$. We use $\Phi$ to present the transition rules of the upper limb's motion. These rules are generated from common-sense experiences, which are described as follows:

***Rules*** $\Phi$:

1. IF $\hat{\tau}_i = 0$ ($i$=1,2,3,4)
   THEN $\hat{I}(n+1)$ is "Stop".
2. ELSE IF $\hat{\tau}_1 \neq 0$ AND $\hat{\tau}_i = 0$ ($i$=2,3,4), OR
   $\hat{\tau}_2 \neq 0$ AND $\hat{\tau}_i = 0$ ($i$=1,3,4), OR
   $\hat{\tau}_3 \neq 0$ AND $\hat{\tau}_i = 0$ ($i$=1,2,4), OR
   $\hat{\tau}_4 \neq 0$ AND $\hat{\tau}_i = 0$ ($i$=1,2,3)
   THEN $\hat{I}(n+1)$ is "Bending and stretching around single joint".
3. ELSE IF $\hat{\tau}_4 \cdot \hat{\tau}_2 < 0$ AND $\hat{\tau}_1 = 0$ AND $\hat{\tau}_3 = 0$
   THEN $\hat{I}(n+1)$ is "Moving straight" OR "Moving along an arc".
4. ELSE $\hat{I}(n+1)$ is "Moving along an arc".

The fuzzy threshold detection methods are used to check which rule should be selected when a transition occurs.

Although the IRD is explicitly described by the direction of resultant desired velocity $\hat{V}_h$, it is subject to the effect of noisy measure force signals. In order to get an accurate IRD, filter technology is one of the good choices. In different motion modes of upper limb, the IRD is described by different models. It should be pointed out that filter technology is necessary only in mode III and mode IV. It is obvious that the IRD is meaningless in a "Stop" mode. Meanwhile, it can be described by a circular trajectory exactly during mode II.

For the state and observation models (3) and (21), the Kalman filter is very suitable to extract the IRD and is chosen in our study. Note that a low dimension Kalman filter is needed in mode III while a high dimension Kalman filter is needed in mode IV to get rid of the effect of measurement noise in the IRD. This is caused by the different state variables in the two modes. Unfortunately, we cannot distinguish mode III and mode IV according to rule $\Phi$-3. That is to say, the exact switching time of the two filters cannot be detected under the condition of $\Phi$-3. To solve this problem, we assume a variable dimension (VD) Kalman filter to infer the IRD in this case. The VD Kalman filter is able to detect the sudden maneuver in a target tracking problem [11].

To conclude the above discussion, the IRD can be online estimated by the following algorithm:

***Algorithm 1***.

Input: $\hat{I}(n)$, $\hat{\tau}_i$
  Switch $\hat{\tau}_i$
    case $\Phi$-1: $\tilde{S}(n) = \langle 0, 0 \rangle$
    case $\Phi$-2: $\tilde{S}(n) = \langle \rho_{o1}(n), \rho_{o2}(n) \rangle$
    case $\Phi$-3: use the VD Kalman filter to infer $\tilde{S}(n)$
    case $\Phi$-4: use the high dimensional Kalman filter to infer $\tilde{S}(n)$
Output: $\tilde{S}(n)$

## III. Intention-Guided Admittance Control for Upper Limb Power-Assist Exoskeleton

In order to make the user feel comfortable while moving his/her arm assisted by the robotic exoskeleton, an IRD guided admittance control strategy is proposed. In this control strategy the admittance model is given by

$$V_h(s) = \frac{1}{Ms + B} \cdot F_{in}(s) \quad (23)$$

where the output $V_h(s)$ is the reference velocity of the hand. The input $F_{in}(s)$ has the same direction as the estimated IRD $\tilde{S}(n)$ and satisfies

$$\|F_{in}\| = \|\hat{V}_h\|. \quad (24)$$

$M$ and $B$ are the mass and the dumping parameters.

Given the reference hand velocity $V_h(s)$, the reference velocities of each joint of robot can be computed by using the inverse Jacobian matrix of the power-assist robotic exoskeleton. These joint reference velocities are fed into the motion controllers of different DOF to control the rotation of DC motors. The whole control system structure is illustrated as the following figure.

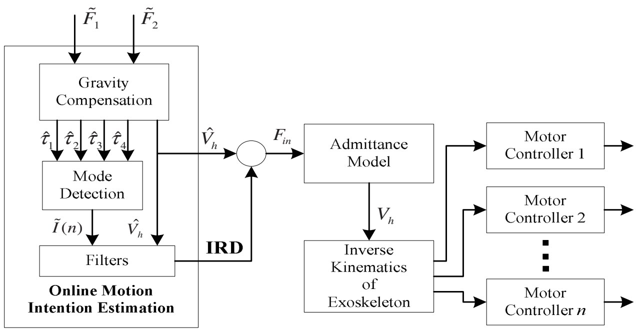


Fig. 5. The control system structure

## IV. Experiments

### A. Setup

A 3-DOF power-assist robotic exoskeleton is designed to test our control approach, which is shown in Fig.6. There are two joints in the shoulder and one joint in the elbow. The actuator for the robotic exoskeleton is DC servo motor. In all the experiments, a subject (male, age 23) is requested to move his arm while wearing the exoskeleton.

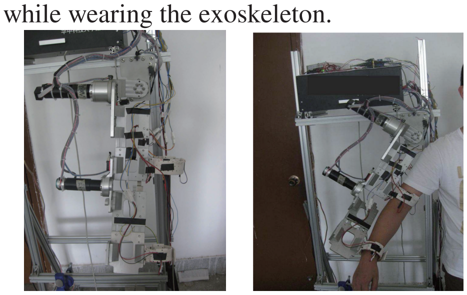

Fig.6. The power-assist robotic exoskeleton.

### B. Experiment of identifying $d_i$

An important prerequisite of the correctness of our method is that assumption 5 and 6 should hold. To validate these assumptions, we first carried out an experiment to identify coefficients $d_i$ given in (14). In this experiment, the subject is requested to move his hand slightly to some given IRDs while the exoskeleton is kept on some fixed posture. In this way, a sample set comprised of $\hat{\tau}_i$ and the direction of $\hat{V}_h$ (i.e. the IRD) can be collected. The problem is the amplitude of $\hat{V}_h$ is unknown. From (14) and (15) we have

$$\overline{\hat{V}_h} = J_h \cdot diag\left(\frac{d_1}{\|\hat{V}_h\|}, \frac{d_2}{\|\hat{V}_h\|}, \frac{d_3}{\|\hat{V}_h\|}, \frac{d_4}{\|\hat{V}_h\|}\right) \cdot [\hat{\tau}_1 \quad \hat{\tau}_2 \quad \hat{\tau}_3 \quad \hat{\tau}_4]^{\mathrm{T}} \quad (25)$$

where $\|\hat{V}_h\|$ and $\overline{\hat{V}_h}$ are used to denote the amplitude of $\hat{V}_h$ and the unit vector along the IRD. Because $\|\hat{V}_h\|$ is not easy to know, from (25) we can calculate $d_2/d_1$, $d_3/d_1$ and $d_4/d_1$ respectively. The experiment results are given in TABLE II. The results meet the assumptions very well.

TABLE II. MEASUREMENT OF $d_i$ ($i$=1,2,3,4)

| Posture | | | IRD | $d_1/d_1$ | $d_2/d_1$ | $d_3/d_1$ | $d_4/d_1$ |
|---|---|---|---|---|---|---|---|
| $\theta_1$ | $\theta_2$ | $\theta_4$ | | | | | |
| 0° | -71.5° | 49.5° | (0, -1, 2.74) | 1 | 1 | 3.26 | 3.26 |
| 0° | -66.9° | 56.4° | (0, -1, 2) | 1 | 1 | 3.11 | 3.11 |
| 0° | -71.5° | 40.9° | (0, -1, 2.43) | 1 | 1 | 2.56 | 2.56 |
| 0° | -68.9° | 46.5° | (0, -1, 2.95) | 1 | 1 | 2.92 | 2.92 |

### C. Upper limb motion experiments guided by IRD

In order to illustrate the validity of the proposed approaches, the subject implemented two series of motion modes while wearing the power-assist robotic exoskeleton controlled by the IRD-guided admittance control method.

First, the subject was requested to perform a series of motions, Stop→Flexion of elbow→Stop→Abduction of shoulder→Stop→Extension of elbow→Stop→Adduction of shoulder, which all belong to mode II except for the mode "Stop". Then, the measured toques $\hat{\tau}_i$ ($i$=1,2,3,4) satisfy the rule $\Phi - 1$ or $\Phi - 2$ (see Fig.7), the toques $\hat{\tau}_i$ ($i$=2, 3) are all almost zero. The inferred modes conform to the subject's motion intention accurately. The trajectories of the inferred mode are shown in Fig.7. The robot arm can assist the subject to realize the motion along the IRD, the angles of joints of the upper limb are also shown in Fig.7.

Second, the subject was requested to perform a series of motions, Stop→Extension of shoulder and Extension of elbow to move his hand along an arc→Extension of shoulder and Extension of elbow to move his hand straight. The inferred IRD $\tilde{S}(n) = \langle \rho_{s1}(n), \rho_{s2}(n) \rangle$, and the observations $\hat{S}(n) = \langle \rho_{o1}(n), \rho_{o2}(n) \rangle$ are shown in Fig.8. Because the torques $\hat{\tau}_i$ ($i$=1,2,3,4) satisfy rule $\Phi - 3$, VD-Kalman filter were used. Based on the VD-Kalman filter, mode III and mode IV can be distinguished very well. The robot arm's motions conform to the human motion intention very well guided by IRD. Trajectories of the inferred mode are also shown in Fig.8. Note that the effectiveness of the Kalman filter is not very well when it just begins working (see Fig.8). That is because the initial dimension of the VD-Kalman filter is low while the motion of the upper limb is in mode IV.

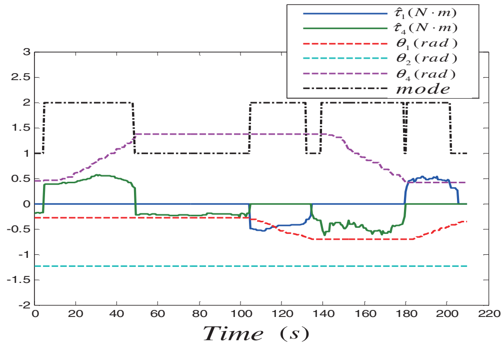

Fig.7. Motion of the upper limb in a series of modes (I→II→I→II→I→II→I→II→I).

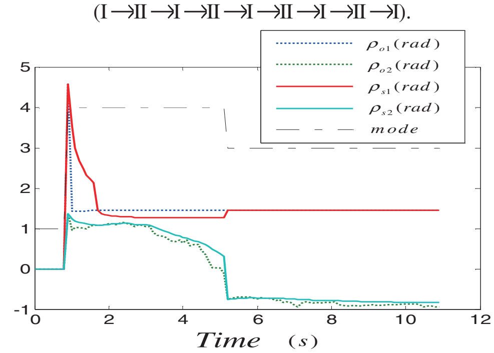

Fig.8. Motion of the upper limb in modes (I→IV→III).

### D. Comparison study

To illustrate the advantages of our methods, a comparison experimental study was performed. In this study, the subject was requested to perform a motion of mode III (Moving straight). Both the proposed IRD-guided control strategy and a normal admittance control strategy without the guidance of IRD were tested. As shown by Fig.9, the norm of the residuals between the trajectory in the case of using normal admittance control and its best fitting line is 24.8, while that between the trajectory in the case of using our IRD-guided control and its best fitting line is 8.5. The hand movement trajectory in the case of using our IRD-guided control is much smoother than the trajectory when using normal admittance control. More than 100 similar trials are performed, and the results are also similar. Accordingly, the subject felt more convenient and comfortable to move his arm while wearing the exoskeleton in the case of using the IRD-guided control strategy.

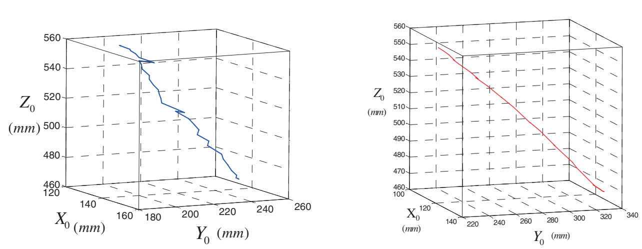

(a) (b)

Fig.9. (a) .The motion trajectory of the hand in the "moving straight" mode without the guided by IRD; (b). The motion trajectory of the hand in the "moving straight" mode with the guided by IRD.

## V. Conclusion

In this paper, an intentional reaching direction (IRD)-guided control strategy for upper-limb power-assist exoskeleton based on online estimating the user motion intention is proposed. The main contribution of this study includes:

*1)* introducing the quantitative definition of human motion intention in the control of upper-limb power-assist robots;

*2)* proposing a systematic modeling and estimation approach for the motion intention;

*3)* applying the online estimated intention to guide the real-time control of robot.

Experimental results show that the proposed control method has many benefits over the conventional admittance control which is often used as a human robot interface (HRI). This control method holds a prospect to be used to design more comfortable human-centered HRI for power-assist robots or rehabilitation robots in the future.

## References


[1] K. Kasaoka, Y. Sankai, "Predictive control estimating operator's intention for stepping-up motion by exo-skeleton type power assist system HAL," in Proc. 2001 IEEE/RSJ International Conference on Intelligent Robots and Systems, Hawaii, USA, Oct., 2001, pp. 1578-1583.

[2] T. Hayashi, H. Kawamoto, Y. Sankai, "Control method of robotic suit HAL working as operator's muscle using biological and dynamical information," in Proc. 2005 IEEE/RSJ International Conference on Intelligent Robots and Systems, pp. 3455-3460.

[3] H. Kawamoto, S. Kanbe, Y. Sankai, "Power Assist Method for HAL-3 Estimating Operator's Intention Based on Motion Information," Proceeding of the 2003 IEEE International Workshop on Robots and Human Interactive Communication, Millbrae, California, USA, Oct. , 2003, pp. 67-72.

[4] K. Yamamoto, M. Ishi, H. Noborisaka, K. Hyodo, "Stand Alone Wearable Power Assisting Suit - Sensing and Control Systems -," in Proceeding of the 2004 IEEE International Workshop on Robot and Human Interactive Communication, Kurashiki, Okayama Japan, Setptember, 2004, pp. 661-666.

[5] F. Chen, Y. Yu, Y. Ge, J. Sun, X. Deng, "WPAL for Enhancing Human Strength and Endurance during Walking," in Proceedings of the 2007 International Conference on Information Acquisition, Jeju City, Korea, July, 2007, pp. 487-491.

[6] J. Rosen, M. Brand, M. B. Fuchs, and M. Arcan, "A Myosignal-Based Powered Exoskeleton System", IEEE Trans. Systems, Man, Cybernetics-Part A: Systems and Humans, vol. 31, no. 3, 2001. pp. 210-222.

[7] K. Kiguchi, T. Tanaka, and T. Fukuda, "Neuro-Fuzzy Control of a Robotic Exoskeleton With EMG Signals," IEEE Trans. Fuzzy Systems, vil. 12, no. 4, pp. 481-490, 2004.

[8] K. Kiguchi, K. Iwami, M. Yasuda, K. Watanabe, and T. Fukuda "An Exoskeletal Robot for Human Shoulder Joint Motion Assist," IEEE/ASME Trans. Mechatronics, vol. 8, no. 1, pp. 125-135, 2003.

[9] J. Huang, P. Di, T. Fukuda, and T. Matsuno, "Motion Control of Omni-Directional Type Cane Robot Based on Human Intention," in Proc. IEEE/RSJ International Conference on Intelligent Robots and Systems, Nice, France, 2008, pp.273-278.

[10] J. J. Craig, "Introduction to Robotics Mechanics and Control," Addison-Wesley Publishing Company, USA, 1989.

[11] Y. Bar-Shalom, K. BIRMIWAL, " Variable Dimension Filter for Maneuvering Target Tracking," IEEE Trans Aerospace and Electronic Systems, vol. aes-18, no.5, 1982, pp.621-629.